





Please cite the Published Version

Ferreira, B , Arantes, IVS, Crapnell, RD , Bernalte, E, Banks, CE  and Paixao, TRLC 
(2025) 3D printing pen for patterning electrochemical sensors on a paper platform for capsaicin detection. Analyst. ISSN 0003-2654

DOI: <https://doi.org/10.1039/d4an01382d>

Publisher: Royal Society of Chemistry (RSC)

Version: Accepted Version

Downloaded from: <https://e-space.mmu.ac.uk/638230/>

Usage rights:  [Creative Commons: Attribution 4.0](https://creativecommons.org/licenses/by/4.0/)

Additional Information: This is an author-produced version of the published paper. Uploaded in accordance with the University's Research Publications Policy

Data Access Statement: Data supporting this article was included as part of the Electronic Supplemental Material

Enquiries:

If you have questions about this document, contact openresearch@mmu.ac.uk. Please include the URL of the record in e-space. If you believe that your, or a third party's rights have been compromised through this document please see our Take Down policy (available from <https://www.mmu.ac.uk/library/using-the-library/policies-and-guidelines>)

3D printing pen for patterning electrochemical sensors on a paper platform for capsaicin detection

Bruno Ferreira,^{a,b} Iana V. S. Arantes,^{a,b} Robert D. Crapnell,^b Elena Bernalte,^b Craig E. Banks^b and Thiago R. L. C. Paixao^{*a}

The development of a print-at-home, low-cost, and miniaturized paper-based cell with 3D-printed electrodes using a 3D-printing pen and a bespoke conductive filament for detecting capsaicin in hot sauce is reported herein. The material cost of producing each electrode was less than £0.01. The new filament was electrochemically benchmarked against a commercial CB/PLA conductive filament. The CB/graphite/recycled PLA filament molded in paper platform produced a heterogeneous rate constant, k_{obs}^0 , of $1.64 (\pm$

$0.13) \times 10^{-3} \text{ cm s}^{-1}$ and resistance of only $166 \pm 0.13 \Omega$ compared to $0.43 (\pm 0.05) \times 10^{-3} \text{ cm s}^{-1}$ and $1613 \pm 220 \Omega$ for an identical device printed from commercial CB/PLA filament. The newly developed device using the bespoke filament on kraft paper was applied successfully to detect capsaicin (CAP). CAP showed a characteristic peak at approximately +0.7 V for the bespoke CB/graphite/rPLA filament in cyclic voltammetry. A small peak at +1.0 V is observed when using the commercial filament. Additionally, a linear range of 5 to 20 μM and a sensitivity of 0.0093 $\mu\text{A } \mu\text{M}^{-1}$ was obtained for CAP when applying differential pulse voltammetry using the paper-based device with the bespoke filament. Limits of detection and quantification were calculated at 1.21 and 3.98 μM , respectively. The new system quantifies CAP in a commercial red pepper hot sauce (Tabasco). This work highlights how a low-cost kraft paper platform and a bespoke conductive filament can be combined to create an effective electrochemical device using simple tools for quantifying capsaicin in real samples. Additionally, it highlights the potential of these materials and techniques to develop home-based sensors.

1. Introduction

Analytical chemistry combines classical, wet chemical, and instrumental methods to separate and identify components within various applications.¹ As such, researchers are constantly pushing to improve or discover new methodologies to maximize the performance of these devices. A wide variety of laboratory-based methods are utilized throughout analytical science, such as atomic spectroscopy, high-performance liquid chromatography, mass spectrometry, and nuclear magnetic resonance spectroscopy. Many of these classical methods involve costly machinery and experienced users and require the sample to be transported to the laboratory. Electrochemical methods offer an alternative approach, with affordable and easy-to-use equipment capable of providing

sensitive results *in situ* in short time frames. Due to these advantages, it is possible to imagine a world where home electroanalytical tests can be carried out despite the electrode development being the most significant limitation. Classical electrodes, such as glassy carbon, are relatively expensive and require surface modification and cleaning after each use. On the other hand, current disposable alternatives, such as screen-printed electrodes, are effectively not viable for home production. However, with the recent revolution of additive manufacturing, particularly fused filament fabrication (FFF), and the availability of commercial conductive filaments, rapid and customized electrode prototyping is now a reality.

FFF functions through the deposition of thermoplastic material in a layer-by-layer fashion to produce a 3D object. This technology allows for on-demand manufacturing, a high degree of customizability, and low waste production compared to its traditional formative and subtractive counterpart.² Additive manufacturing has seen a huge increase in popularity within industry, academia, and home or hobby printers due to the relatively low cost of entry. Nowadays, reliable FFF printers can be purchased for a few hundred GBP, and its closest minimalist concept is the 3D printing pens, which are already

^aDepartment of Fundamental Chemistry, Institute of Chemistry, University of São Paulo, São Paulo, SP, 05508-000, Brazil. E-mail: trlcp@iq.usp.br

^bFaculty of Science and Engineering, Manchester Metropolitan University, Dalton Building, Chester Street, M1 5GD, Great Britain

sold in standard supermarkets for no more than 30–40 GBP. The main advantage of the 3D pen is that no further knowledge about computer-aided design (CAD) is needed, and it allows users to draw a raised graphic and form unique 3D structures instantly. The application of 3D pens has been explored in various studies. de Oliveira *et al.* were the pioneers in using a 3D pen with commercial CB/PLA filament within molds created on a copper board for the simultaneous detection of Cd(II) and Pb(II).³ Pradela-Filho *et al.* utilized a 3D pen with commercial CB/PLA filament, which had been polished with sandpaper, to quantify caffeic acid in tea samples.⁴ Additionally, Lisboa *et al.* employed a novel conductive filament of 40% graphite and 60% PLA, using a 3D pen in conjunction with glassy carbon to quantify the antibiotic ciprofloxacin in pharmaceutical samples and milk.⁵

The availability of conductive filament used in additive manufacturing has led to serious interest within the electrochemical community in producing bespoke accessories,⁶ equipment,⁷ electrodes,⁸ and electroanalytical platforms.^{9–12} Although interesting works have been reported utilizing commercial conductive filament, including many ways to improve it,^{13–21} the electrochemical performance still falls significantly short of where it needs to be to offer a feasible alternative to classical electrodes. As such, researchers have begun to produce their own bespoke filament, which produces significantly better electrochemical performance, while also improving the sustainability of the materials.²² Work in this area started with the inclusion of carbon black (CB) within poly(lactic acid) (PLA), alongside the addition of a plasticizer to help improve the low-temperature flexibility of the filament. These filaments were used for energy storage,²³ environmental electroanalysis,²⁴ and forensic electroanalysis.²⁵ To improve the performance, researchers have begun mixing the conductive fillers incorporated into the filament, such as mixing multi-walled carbon nanotubes with CB,²⁶ metallic particles,²⁷ and graphite.²⁸ These last examples are engaging with the inclusion of graphite. Graphite is a naturally occurring material that remains highly stable and cost-effective under standard conditions. In contrast, carbon black (Super P) is derived from the partial oxidation of petrochemical precursors and can be expensive, with prices reaching up to £300 for just 100 grams. Therefore, substituting carbon black with graphite presents an intriguing opportunity for enhancing the sustainability of electrochemical systems and reducing material costs, all while maintaining comparable electrochemical performance.

Using low-cost substrates, such as paper, PVC, and Kapton tape, to manufacture electrodes has been well-documented in the literature.^{29–31} Paper is the most popular choice among these substrates due to its easy access, flexibility, porosity, and eco-friendly nature.³⁰ Several techniques are utilized to produce carbon devices on low-cost platforms, primarily involving carbon deposition onto the substrate's surface.³² Among these techniques, the best known are pencil drawing, stencil drawing, screen printing, laser scribing, and using a 3D pen.^{4,32,33} 3D pens are a fast way to develop devices using FFF. This equipment can be readily found online and marketed as

a toy, but it can also be used for manufacturing devices.^{3,34} However, the integrated junction of low-cost conductive filament, 3D pen, and paper has never been used in the literature to develop electrochemical devices.

Capsaicin (CAP), a lipophilic alkaloid, is the main compound in chili peppers, contributing to their characteristic spiciness.³⁵ The consumption of CAP can offer health benefits and plays a significant role in combating arthritis and reducing inflammation. However, excessive intake raises concerns, as it may be associated with an increased risk of conditions such as stomach cancer.³⁶ Numerous methods for quantifying capsaicin are documented in the literature, with gas chromatography (GC) and liquid chromatography (LC) being the most employed techniques.^{37,38} However, these methods often involve high equipment costs and significant solvent consumption, making them less suitable for rapid and eco-friendly analyses. Electrochemical techniques present a compelling alternative due to their lower equipment costs, portability, and minimal analysis volume requirements. Typically, only a potentiostat, a three-electrode system (comprising a working electrode, reference electrode, and counter electrode), and data analysis software are necessary for these methods.

Therefore, in this work, we propose using a low-cost graphite/CB mixed filament alongside a 3D printing pen and paper-based mask to produce electroanalytical devices. Using this equipment and material keeps the cost of production low while allowing it to be simple and viable for home production. We look to show how this methodology can produce high-performing and reliable sensors and apply them to the detection of capsaicin within real hot sauce samples, highlighting how this could be used in a home setting.

2. Materials and methods

2.1 Chemicals

Hexaamineruthenium(III) chloride ($[\text{Ru}(\text{NH}_3)_6]^{3+}$) (98%), castor oil, potassium chloride (99.0–100.5%), graphite powder ($<20 \mu\text{m}$), capsaicin standard ($\geq 95\%$, from *Capsicum* sp), sulfuric acid, acetic acid glacial, absolute ethanol, phosphoric acid, hydrochloric acid and sodium hydroxide were purchased from Merck (Darmstadt, Germany). CB was purchased from PI-KEM (Tamworth, UK). Recycled PLA pellets were purchased from Gianeco (Turin, Italy). Commercial conductive CB/PLA filament (1.75 mm, Proto-Pasta, Vancouver, Canada) was purchased from Farnell (Leeds, UK). All solutions were prepared with deionized water of resistivity not less than $18.2 \text{ M}\Omega \text{ cm}$ from a Milli-Q Integral 3 system from Millipore UK (Watford, UK). Tabasco® hot pepper sauce was bought in a São Paulo, Brazil grocery store.

2.2 Conductive filament production

The filament was made as outlined previously.²⁸ Briefly, recycled PLA (rPLA) was dried in an oven at $60 \text{ }^\circ\text{C}$ for a minimum of 2.5 hours before any mixing or filament production. The polymer composition was prepared using 60 wt% rPLA, 10 wt% castor oil, 18 wt% carbon black (CB), and

12 wt% graphite powder. These are mixed (190 °C) with Banbury rotors (70 rpm for 5 min) using a Thermo Haake Polydrive dynamometer fitted with a ThermoHaake Rheomix 600 (Thermo-Haake, Germany). The resultant composite is allowed to cool to room temperature before being granulated to create a finer granule size using a (Rapid Granulator 1528). This is next processed through an EX2 extrusion line (Filabot, VA, United States) using a single screw with a heat zone of 190 °C, which is extruded from a 1.75 mm die head. Then, the filament is ready to use for additive manufacturing/3D-printing. It is important to highlight that the filament proposed in this work has a smaller amount of wt% CB (18%) than the commercial filament used (~21%) and uses graphite for the remaining carbon, which is more sustainable.

2.3 Conductive filament characterization

All electrochemical measurements were performed with a Metrohm Autolab PGSTAT204 potentiostat/galvanostat controlled by NOVA 2.1.6 (Utrecht, the Netherlands). The electrochemical characterization of the bespoke filament and comparison to the benchmark were performed on a lollipop shape electrode developed using a 3D printing pen on a stencil design produced on kraft paper using a CO₂ laser machine. The working electrode was made of CB/graphite/rPLA filament, and the reference and counter electrodes were 3D printed with a commercial CB/PLA filament. The electrochemical characterization was carried out using the cyclic voltammetry (CV) technique with a 1 mM [Ru(NH₃)₆]Cl₃ solution. Before each experiment, the solution was deoxygenated using N₂. Electrochemical impedance spectroscopy (EIS) was performed at 10⁵ and 10⁻¹ Hz frequencies at -0.16 V vs. CB/PLA with an amplitude of 10 mV.

Scanning electron microscopy (SEM) measurements were recorded on a Supra 40VP Field Emission (Carl Zeiss Ltd, Cambridge, UK) with an average chamber and gun vacuum of 1.3 × 10⁻⁵ and 1 × 10⁻⁹ mbar, respectively. Samples were mounted on the aluminium SEM pin stubs (12 mm diameter, Agar Scientific, Essex, UK). To enhance the contrast of these images, a thin layer of Au/Pd (8 V, 30 s) was sputtered onto the electrodes with the SCP7640 from Polaron (Hertfordshire, UK) before being placed in the chamber.

2.4 Electrochemical paper-based analytical device (ePAD) fabrication

A kraft paper sheet was first waterproofed with a varnish waterproof spray, and then cut using a CO₂ laser cutter (work special laser) in the desired geometry (RDWorks 8.0) to create a mask. The kraft paper mask was placed upside down on a flat surface and secured with adhesive tape to prevent movement during electrode fabrication. Using a 3D printing pen, the mask was filled with conductive filaments. The filaments were applied roughly and then pressed firmly to ensure an even distribution within the designated spaces for the electrodes. Afterward, the device was turned back to its original side, with the electrodes facing up, remaining aligned with the paper. Finally, the hydrophobic barrier was manually drawn with the 3D pen using a non-conductive filament. A 3D print-

ing pen (3Dpen-P62-2-China) with a 0.7 mm nozzle and an extrusion temperature set to 190 °C was utilized to extrude the filaments. The working electrode (WE) area (2 mm diameter) was filled with the bespoke CB/graphite/rPLA filament (~0.03 g). In contrast, the reference (RE) and counter (CE) electrodes were filled with a commercial CB/PLA filament (~0.05 g). Next, the three-electrode system coupled to the paper was polished in sandpaper (Wetordry 1500) to uniform the electrode's surface. Finally, a reservoir (~200 μL) was also designed around the electrodes using the 3D-printing pen machine filled with non-conductive PLA filament to confine the solution during the electrochemical measurements (Fig. 1). For the benchmark with the CB/PLA commercial filament, another device was constructed using CB/PLA as a working electrode. The specific process of polishing the electrode surface using sandpaper was carried out on the bespoke CB/graphite/rPLA device and benchmark commercial filament (CB/PLA) device prior to the analyses. For both the bespoke and benchmark devices, the conventional activation using NaOH was not applied, only the surface polishing as previously described. In Fig. S1,† the original image of the device and its construction process can be observed. Fig. S1A† depicts the mask being manufactured using a CO₂ laser. In Fig. S1B,† the device is shown with three electrodes—working electrode (WE), reference electrode (RE), and counter electrode (CE)—along with the filaments. Finally, Fig. S1C† presents the complete device, featuring a barrier of non-conductive filament, three electrodes positioned in the center, and a comparison using a coin to demonstrate the real dimension of the device.

2.5 Capsaicin analysis

First, capsaicin (CAP) stock solutions were prepared daily by dissolving capsaicin powder in absolute ethanol. Subsequently, capsaicin standard solutions were adequately diluted in the different

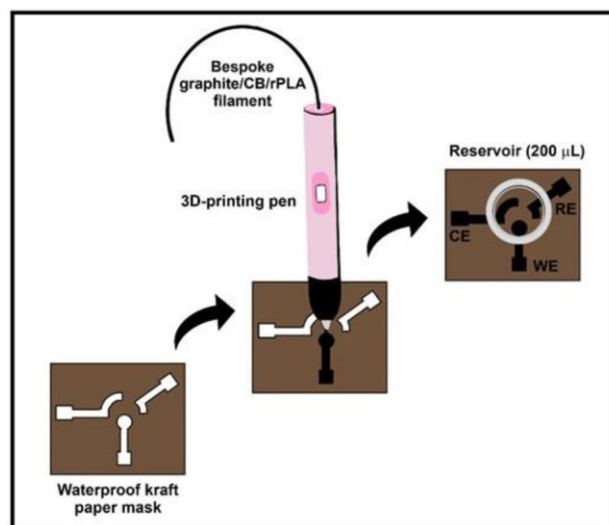


Fig. 1 Schematic representation of the ePAD manufacturing process using a 3D-printing pen and the bespoke filament in the WE (RE and CE were made of commercial filament).

supporting electrolytes selected for the optimization of the electroanalytical methodology as well as for the capsaicin analytical procedure performed in 0.12 mol L⁻¹ BR buffer pH 1.³⁹ The ePAD fabricated with the bespoke filament was applied to quantify CAP in a commercial red pepper sauce (Tabasco®). The procedure of capsaicin extraction was carried out according to the literature.³⁹ Briefly, the red pepper sauce (200 mg) was mixed in the ethanol solvent (5 mL), sonicated for 60 minutes, and filtered with a standard funnel using a Whatman filter paper No 42 (pore diameter of 125 μm). The solution was properly diluted (1.5-fold) in the supporting electrolyte and spiked with known capsaicin concentrations. The standard addition method was chosen to determine the concentration of CAP in the Tabasco pepper sauce.

3. Results and discussion

3.1 Electrochemical characterization of the ePAD

The electrochemical performance of the bespoke CB/graphite/rPLA and the commercial CB/PLA filaments were tested using a 3D-printing pen for directly extruding the filaments into the kraft paper mold to create the three-electrode system. Note that in this work the working electrodes utilized ~0.03 g of material, meaning the material cost of using the bespoke filament was less than 1 pence per electrode. The near-ideal outer-sphere redox probe [Ru(NH₃)₆]³⁺ (1 mM in 0.1 M KCl) was used for all characterization experiments, comparing the bespoke and the commercial filaments used as working electrodes, respectively. Initially, the ePAD device fabricated using the bespoke CB/graphite/rPLA was tested using cyclic voltammetric (CV) scan rate studies (5–500 mV s⁻¹), as seen in Fig. 2A. This allows for the best determination of the heterogeneous electrochemical rate constant (k_{obs}^0) and the real electrochemical surface area of the electrodes (A_e).⁴⁰ A comparison of the CV response to [Ru(NH₃)₆]³⁺ at 100 mV s⁻¹ from the bespoke CB/graphite/rPLA filament and the commercially purchased CB/PLA filament, is presented in Fig. 2B. A summary of the electrochemical parameters is included in Table 1 demonstrating that WE from the bespoke filament within the novel ePAD configuration is outperforming the commercial CB/PLA filament, where a cathodic peak current (I_p^c) is ~4 times higher and a significant reduction in the peak-to-peak separation (ΔE_p) is observed for the bespoke electrode. Additionally, the calculated values for k^0

and A_e

obs

are summarized in Table 1 were also higher for the bespoke CB/graphite/rPLA, highlighting the enhanced performance of the bespoke filament.

Fig. 2C shows the Nyquist plots obtained from electrochemical impedance spectroscopy (EIS) measurements (100 000–0.1 Hz) in 1 mM [Ru(NH₃)₆]³⁺ (0.1 M KCl). As summarized in Table 1, the CB/graphite/rPLA filament performed well with a charge transfer resistance (R_{ct}) of 9.7 ± 1.4 kΩ compared to 27.7 ± 3.7 kΩ for the commercial filament.

It is important to emphasize that the characterization of the CB/graphite/rPLA filament indicates the electrochemical performance is vastly improved when compared to the commercially available filament even though the filament made in

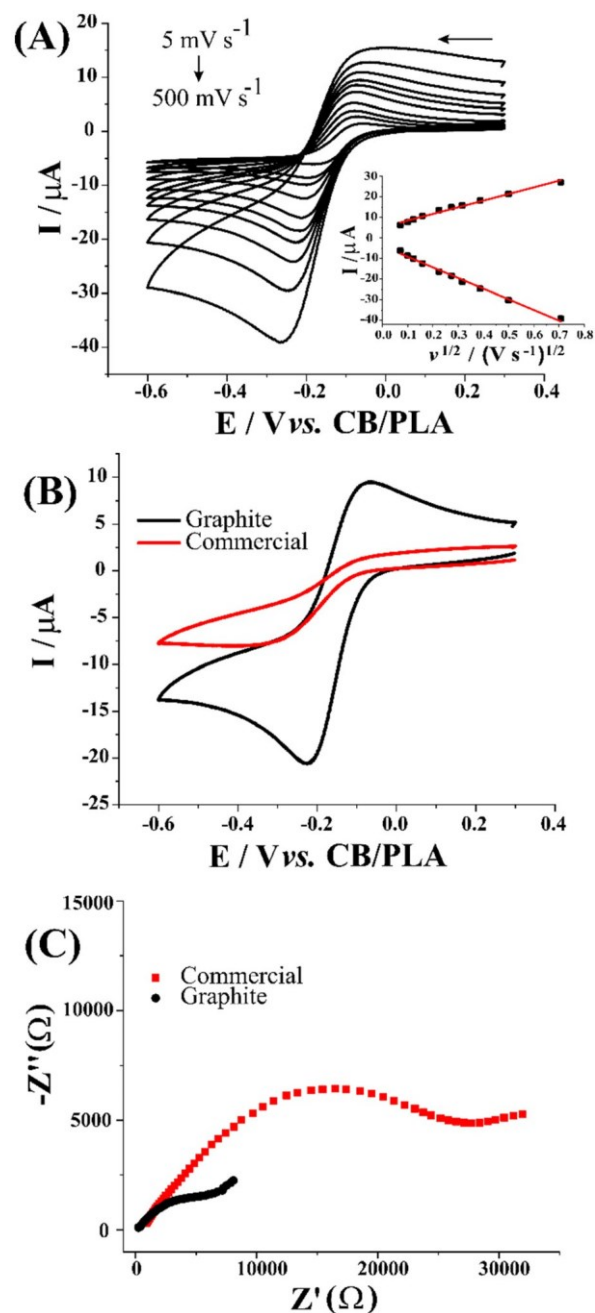


Fig. 2 (A) Cyclic voltammograms (5–500 mV s⁻¹) of [Ru(NH₃)₆]³⁺ (1 mM in 0.1 M KCl) with the CB/graphite/rPLA filament as the WE and the

commercial filament as CE and RE in the ePAD. The Randles-Sevcik plot is presented inset. (B) Comparison of the CVs (100 mV s⁻¹) of [Ru(NH₃)₆]³⁺ (1 mM in 0.1 M KCl) for the CB/graphite/rPLA and the commercial electrodes. (C) Nyquist plot of [Ru(NH₃)₆]³⁺ (1 mM in 0.1 M KCl), performed in the CB/graphite/rPLA and the commercial electrodes.

the laboratory contains less carbon black and a greater amount of graphite in its structure. Another important point is that the amount of graphite drastically reduces material costs when compared to a CB only filament of the same loading.⁴¹ Fig. S2† shows the SEM analyses of bespoke CB/graphite/rPLA recorded at different magnifications, facilitating to visualiza-

Table 1 Comparisons of the averages ($N = 2$) of cathodic peak currents ($-I_p^c$), peak-to-peak separations (ΔE_p), heterogeneous electron transfer constant (k_{obs}^0), electrochemically active area (A_e), EIS charge transfer resistance (R_{ct}) and solution resistance (R_s), and the surface resistance (R) of the working electrode for the graphite and the commercial filament

Parameter	CB/graphite/rPLA	Commercial CB/PLA
$-I_p^c$ (mA) ^a	28.2 ± 9.5	7.44 ± 0.60
ΔE_p (mV)	149 ± 6	315 ± 17
k_{obs}^0 (cm ² s ⁻¹) ^b	$(1.64 \pm 0.13) \times 10^{-3}$	$(0.43 \pm 0.05) \times 10^{-3}$
A_e (cm ²)	0.11 ± 0.03	0.04 ± 0.01
R_{ct} (k Ω)	9.7 ± 1.4	27.7 ± 3.7
R_s (Ω) ^c	222 ± 86	1800 ± 1000
R (Ω) ^d	166 ± 13	1613 ± 220

^a Extracted from 100 mV s⁻¹ CVs of [Ru(NH₃)₆]³⁺ (1 mM in 0.1 M KCl).

^b Calculated from the [Ru(NH₃)₆]³⁺ scan rate study (5–500 mV s⁻¹).

^c Extracted from Nyquist plots of EIS experiments in a solution of [Ru(NH₃)₆]³⁺ (1 mM in 0.1 M KCl). ^d Resistance measured with a multimeter.

tion of the microstructure of the bespoke filament combining graphite flakes with smaller dots of CB, as observed more clearly in Fig. S2C and D.†

The reproducibility and repeatability of the CB/graphite/PLA device were assessed. Fig. S3A† presents voltammograms from seven different electrodes, demonstrating a relative standard deviation (RSD) of 5.5% for the I_p^c . In Fig. S3B,† thirteen cyclic voltammograms from the same electrode are displayed, with the results showing an RSD of 5.6% for I_p^c . All experiments were conducted using a solution of 1 mM [Ru(NH₃)₆]³⁺ in 0.1 M KCl.

3.2 Electroanalytical determination of capsaicin

The ePAD fabricated with the CB/graphite/rPLA filament was tested for capsaicin (CAP) detection. Fig. 3A shows the CVs,

where it is possible to see two oxidation peaks, *i.e.*, peak I (~0.8 V) and peak III (~0.6 V), and a reduction peak, *i.e.*, peak II (~0.1 V). According to the literature, the capsaicin oxidation process is relatively complex, and two other processes occur at

the electrode in an acidic medium. These processes can be observed starting in the first cycle, red voltammogram of Fig. 3A, where the guaiacol ring of capsaicin molecule oxidation occurs in peak I (~0.8 V) to an intermediate. In the reduction process, it is possible to see a reduction peak, peak II (~0.1 V), representing the benzoquinone reduction and sub-

sequently an oxidation peak III (~0.6 V) that is the catechol peak, a product of the reduction of benzoquinone. This process for peaks II and III is reversible for these two molecules in the electrode surface, while peak I, referring to capsaicin oxidation, occurs irreversibly on the surface of the electrode. It is important to highlight that the capsaicin oxidation peak decreases through the cycles while the catechol oxidation peak increases (cycle 1 to cycle 2).^{39,42,43}

The comparison between CB/graphite/rPLA filament and the commercial filament for the detection of capsaicin is shown in Fig. 3B, where the oxidation peak I is more intense in the bespoke filament than in the commercial one, showing better performance for this electrode.

3.3 pH study of capsaicin

Next, the optimal pH for CAP detection was investigated, analyzing the subsequent cyclic voltammograms recorded at different pH values (1 to 10). The CVs depicted in Fig. S4A† show that the highest current peak for capsaicin oxidation at a potential of 0.8 V is obtained in a solution of pH 1.³⁹ This is further confirmed while plotting the peak current (I_p) vs. pH, as Fig. S4B† shows that pH 1 is the most effective for detecting capsaicin. The increase in anodic current with decreasing pH

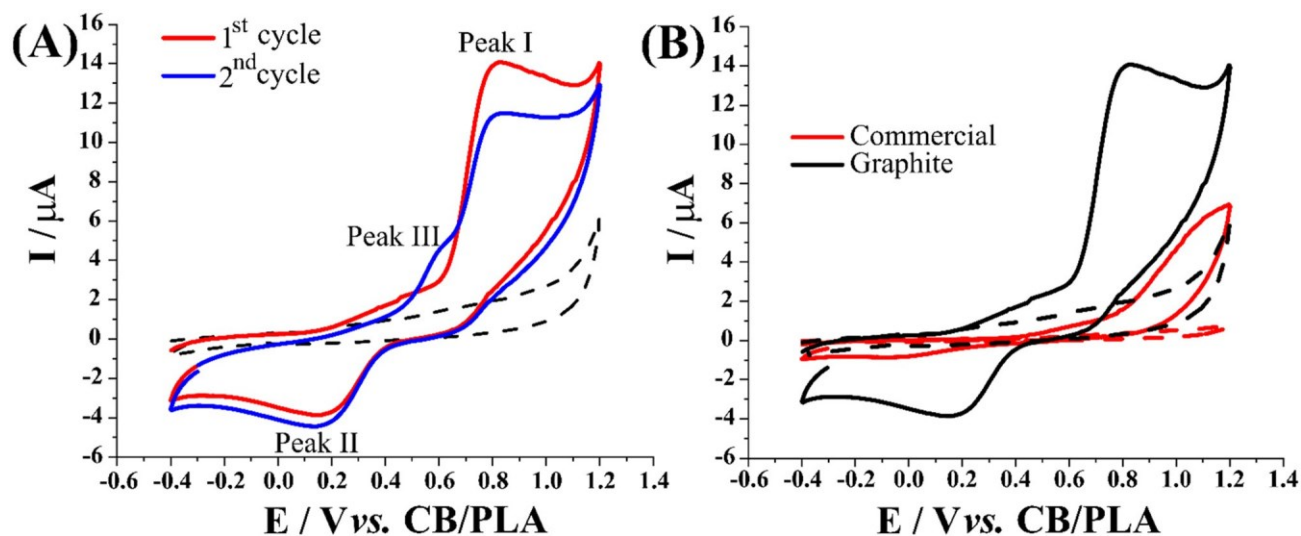


Fig. 3 (A) CVs (100 mV s⁻¹) of 500 μM capsaicin in BR buffer pH 1.0 in the CB/graphite/rPLA. The dashed line represents the blank, red and blue lines are the first and second cycles, respectively. Capsaicin oxidation is exhibited in Peak I, followed by benzoquinone reduction in Peak II, and its

subsequent oxidation of catechol (Peak III), only present in the second cycle. (B) CVs of 500 μM capsaicin (100 mV s^{-1}) in BR buffer pH 1.0 performed in the CB/graphite/rPLA and in the commercial CB/PLA electrode in the ePAD.

is probably due to protonation in the phenolic portion of the capsaicin molecule.⁴² The oxidation peak potential (E_p) and pH relationship were also established for capsaicin detection, as shown in Fig. S4C.† The ratio of protons to electrons was calculated using a pH gradient, and the resulting value for the m/n ratio is 0.52, where m represents the number of protons and n represents the number of electrons. In Fig. S4D,† different supporting electrolytes were tested (0.12 M BR buffer, 0.1 M HCl, and 0.1 M H₂SO₄) and evaluated for capsaicin detection. BR buffer was determined to be the optimal supporting electrolyte for quantifying capsaicin.

Furthermore, a scan rate test (Fig. S5A†) was conducted to help further understand the capsaicin mechanism. Fig. S5B† depicts the peak potential (E_p) and $\ln(\nu)$ relationship. The number of electrons calculated for the Laviron equation from this relationship was ~ 2.16 . Using the m/n value previously obtained in the E_p vs. pH study, it is possible to conclude that the capsaicin mechanism involves 1 proton and 2 electrons, consistent with what was found in the literature.³⁹

3.3 Quantification of capsaicin

The CB/graphite/rPLA and the commercial CB/PLA electrodes 3D-printed on an ePAD device were compared for capsaicin determination using differential pulse voltammetry (DPV). Fig. S6† compares DPV responses for capsaicin between the two electrodes, illustrating the difference in sensitivity to the molecule's signal. It is observed that a small peak is obtained for the commercial filament ePAD at ~ 0.7 V. In contrast, a large and well-defined peak is observed for the bespoke filament ePAD, demonstrating better performance of the bespoke filament in the electroanalytical quantification of capsaicin.

Then, an analytical curve was built for CB/graphite/rPLA electrode to detect capsaicin. Fig. 4A shows the increase in the peak current with capsaicin concentration, and Fig. 4B demonstrates the linearity of the response with capsaicin concentration in the range from 5 to 20 μM (I (μA) = 0.0093 $C_{\text{capsaicin}}$

(μM) + 0.0091); ($R = 0.9985$). Moreover, the CB/graphite/rPLA electrode showed a good limit of detection (LOD) of 1.21 μM

and 3.98 μM limit of quantification (LOQ). The performance of the developed ePAD device using bespoke CB/graphite/rPLA filament was tested for capsaicin quantification in a real sample, namely a commercial red pepper sauce (Tabasco®). Standard addition of capsaicin was performed starting from the sample (red line) up to 30 μM of the standard (black lines), as illustrated in Fig. 4C. The concentration of capsaicin determined from the standard addition curve on red pepper sauce was found to be 3.13 μM , consistent with values previously reported in the literature.³⁹

Table 2 summarizes the research that utilized carbon or carbon-modified working electrodes for capsaicin detection. Notably, this is the first study in the literature to employ a bespoke 3D printing conductive filament combined in a kraft paper platform for fabricating a low-cost ePAD to detect and quantify capsaicin. The LOD and LOQ values are relatively

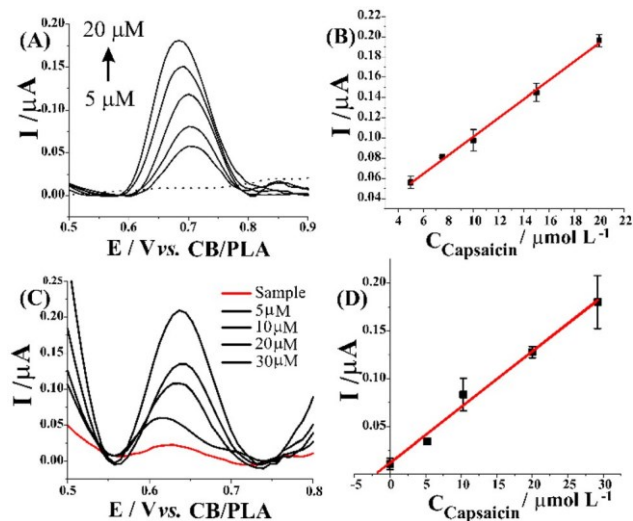


Fig. 4 (A) DPV measurements ($N = 2$) for increasing concentrations of capsaicin (5–20 μM) in BR buffer pH 1.0 performed in the CB/graphite/ rPLA in the ePAD (potential step: 8 mV; amplitude: 50 mV), and (B) the respective calibration curve for capsaicin oxidation ($E = +0.7$ V). (C) DPV measurements of a pepper sauce sample (red line) diluted (1.5 fold) in BR buffer pH 1.0 and spiked with capsaicin standard solutions (5 to 30 μM) (black lines); (D) represents the respective standard addition calibration curve. Potential step: 8 mV; amplitude: 50 mV.

Table 2 A comparison of the analytical parameters of the proposed electroanalytical platform for CAP with other alternatives has been recently reported in the literature

Device	Linear range (μM)	LOD (μM)	Technique	REF
CB-SPE	0.080–6	0.028	DPV	39
SPCE	0.16–16.37	0.05	DPV	43
MWCNT-BPPGE	0.5–35	0.45	CV	42
rGO – SPCE	1.1–25	0.30	CV	44
NH ₂ -FMS/CPE	0.4–4.0	0.020	LSV	45
Ni-CNT/S-rGO/GCE	0.01–100	0.001	DPV	46
CB/graphite/rPLA ePAD	5–20	1.21	DPV	This work

high when compared with other works in the literature. However, given the relatively high concentration of capsaicin

CB-SPE – carbon black-printed electrode; SPCE – screen-printed carbon electrode; GCE – glassy carbon electrode; MWCNT-BPPGE – multiwalled carbon nanotube modified basal plane pyrolytic graphite electrode; rGO – SPCE – screen-printed carbon electrode with reduced graphene oxide; NH₂-FMS/CPE – amino-functionalized mesoporous silica/carbon paste electrode; Ni-CNT/S-rGO/GCE – nickel nanoparticles modified carbon nanotube and sulfonated reduced graphene oxide with glassy carbon electrode; DPV – differential pulse voltammetry; SWV – square wave voltammetry; LSV – linear sweep voltammetry.

in pepper samples, this is a minor concern. Another important aspect to consider is the cost of the device in the literature. This study utilized low-cost filament, a material cost of £58.50 per kg, without modification, and a paper platform, resulting in an affordable, portable, and rapidly fabricated device. Additionally, the accessibility and affordability of the 3D printing pen compared to a regular 3D printing machine make it a practical choice for print-at-home devices.

4. Conclusion

Using low-cost filaments made from CB, graphite, castor oil, and rPLA in conjunction with 3D pen machines for an innovative paper-based design marks a significant advancement. This innovative approach involves using kraft paper as a template to apply the new filament, resulting in superior electrochemical performance compared to devices made with commercial filament. Notably, including graphite in the filament structure reduces costs while increasing the overall carbon loading and, therefore, the electrochemical kinetics, leading to

higher values of k_{obs}^0 and current for both probes and the

analyte. The material cost of producing each electrode was less than 1 pence. The utilization of a 3D pen for analytical applications has proven to be a significant development as it eliminates the need for a conventional 3D printer to create complete 3-electrode.

Author contributions

Conceptualization and investigation: BF and IVSA; methodology: BF and IVSA; writing – original draft: BF, EB, and RDC; writing – review & editing: all authors; supervision and funding acquisition: CEB and TRLCF.

Data availability

Data supporting this article was included as part of the ESI.†

Conflicts of interest

There are no conflicts to declare.

Acknowledgements

This research was supported by São Paulo Research Foundation (FAPESP) (Grant number: 2023/00246-1 and 2019/15065-7), Coordenação de Aperfeiçoamento de Pessoal de Nível Superior – Brasil (CAPES) (Grant numbers: 88887.601733/2021-00 and Finance Code 001), Conselho Nacional de Desenvolvimento Científico e Tecnológico (Grant number: 311847-2018-8 and 302839/2020-8).

References

- 1 A. García-Miranda Ferrari, S. J. Rowley-Neale and C. E. Banks, *Talanta Open*, 2021, 3, 100032.
- 2 M. Attaran, *Int. J. Res. Eng. Sci.*, 2016, 4, 30–38.
- 3 F. M. de Oliveira, E. I. de Melo and R. A. B. da Silva, *Sens. Actuators, B*, 2020, 321, 128528.
- 4 L. A. Pradela-Filho, W. B. Veloso, D. N. Medeiros, R. S. O. Lins, B. Ferreira, M. Bertotti and T. R. L. C. Paixão, *Anal. Chem.*, 2023, 95, 10634–10643.
- 5 T. P. Lisboa, L. V. de Faria, W. B. V. de Oliveira, R. S. Oliveira, M. A. C. Matos, R. M. Dornellas and R. C. Matos, *Microchim. Acta*, 2023, 190, 310.
- 6 M. J. Whittingham, R. D. Crapnell, E. J. Rothwell, N. J. Hurst and C. E. Banks, *Talanta Open*, 2021, 4, 100051.
- 7 M. J. Whittingham, R. D. Crapnell and C. E. Banks, *Anal. Chem.*, 2022, 94, 13540–13548.
- 8 A. Garcia-Miranda Ferrari, N. J. Hurst, E. Bernalte, R. D. Crapnell, M. J. Whittingham, D. A. C. Brownson and C. E. Banks, *Analyst*, 2022, 147, 5121–5129.
- 9 R. M. Cardoso, C. Kalinke, R. G. Rocha, P. L. dos Santos, D. P. Rocha, P. R. Oliveira, B. C. Janegitz, J. A. Bonacin, E. M. Richter and R. A. A. Munoz, *Anal. Chim. Acta*, 2020, 1118, 73–91.
- 10 A. A. Dias, T. M. G. Cardoso, C. L. S. Chagas, V. X. G. Oliveira, R. A. A. Munoz, C. S. Henry, M. H. P. Santana, T. R. L. C. Paixão and W. K. T. Coltro, *Electroanalysis*, 2018, 30, 2250–2257.
- 11 R. D. Crapnell and C. E. Banks, *Anal. Methods*, 2024, 16, 2625–2634.
- 12 R. D. Crapnell, E. Bernalte, A. G. M. Ferrari, M. J. Whittingham, R. J. Williams, N. J. Hurst and C. E. Banks, *ACS Meas. Sci. Au*, 2022, 2, 167–176.
- 13 E. Bernalte, R. D. Crapnell, O. M. A. Messai and C. E. Banks, *ChemElectroChem*, 2024, 11, 1–10.
- 14 M. P. Browne, F. Novotný, Z. Sofer and M. Pumera, *ACS Appl. Mater. Interfaces*, 2018, 10, 40294–40301.
- 15 R. D. Crapnell, A. Garcia-Miranda Ferrari, M. J. Whittingham, E. Sigley, N. J. Hurst, E. M. Keefe and C. E. Banks, *Sensors*, 2022, 22, 9521.
- 16 C. Kalinke, N. V. Neumsteir, G. D. O. Aparecido, T. V. D. B. Ferraz, P. L. Dos Santos, B. C. Janegitz and J. A. Bonacin, *Analyst*, 2020, 145, 1207–1218.
- 17 C. Miller, O. Keattch, R. S. Shergill and B. A. Patel, *Analyst*, 2024, 149, 1502–1508.
- 18 D. P. Rocha, R. G. Rocha, S. V. F. Castro, M. A. G. Trindade, R. A. A. Munoz, E. M. Richter and L. Angnes, *Electrochem. Sci. Adv.*, 2022, 2, 1–15.
- 19 R. S. Shergill, C. L. Miller and B. A. Patel, *Sci. Rep.*, 2023, 13, 339.
- 20 R. S. Shergill and B. A. Patel, *ChemElectroChem*, 2022, 9, 1–8.
- 21 R. S. Shergill, F. Perez, A. Abdalla and B. A. Patel, *J. Electroanal. Chem.*, 2022, 905, 115994.
- 22 L. R. G. Silva, L. V. Bertolim, J. S. Stefano, J. A. Bonacin, E. M. Richter, R. A. A. Munoz and B. C. Janegitz, *Electrochim. Acta*, 2025, 513, 145566.
- 23 P. Wuamprakhon, R. D. Crapnell, E. Sigley, N. J. Hurst, R. J. Williams, M. Sawangphruk, E. M. Keefe and C. E. Banks, *Adv. Sustainable Syst.*, 2023, 7, 2200407.
- 24 R. D. Crapnell, I. V. S. Arantes, M. J. Whittingham, E. Sigley, C. Kalinke, B. C. Janegitz, J. A. Bonacin,

- T. R. L. C. Paixão and C. E. Banks, *Green Chem.*, 2023, 25, 5591–5600.
- 25 I. V. S. Arantes, R. D. Crapnell, M. J. Whittingham, E. Sigley, T. R. L. C. Paixão and C. E. Banks, *ACS Appl. Eng. Mater.*, 2023, 1, 2397–2406.
- 26 C. Kalinke, R. D. Crapnell, E. Sigley, M. J. Whittingham, P. R. de Oliveira, L. C. Brazaca, B. C. Janegitz, J. A. Bonacin and C. E. Banks, *Chem. Eng. J.*, 2023, 467, 143513.
- 27 E. Koukouviti, A. Economou and C. Kokkinos, *Adv. Funct. Mater.*, 2024, 34, 2402094.
- 28 K. K. L. Augusto, R. D. Crapnell, E. Bernalte, S. Zighed, A. Ehamparanathan, J. L. Pimlott, H. G. Andrews, M. J. Whittingham, S. J. Rowley-Neale, O. Fatibello-Filho and C. E. Banks, *Microchim. Acta*, 2024, 191, 3–14.
- 29 B. Ferreira, I. V. S. Arantes, D. P. M. Saraiva, L. A. Pradela-Filho, M. Bertotti and T. R. L. C. Paixão, *Microchem. J.*, 2024, 198, 110149.
- 30 I. V. S. Arantes, J. L. M. Gongoni, L. F. Mendes, V. N. de Ataíde, W. A. Ameku, P. T. Garcia, W. R. de Araujo and T. R. L. C. Paixão, *Paper-based Analytical Devices for Chemical Analysis and Diagnostics*, Elsevier, 1st edn, 2022, pp. 81–116.
- 31 L. F. Mendes, A. de Siervo, W. Reis de Araujo and T. R. L. C. Paixão, *Carbon*, 2020, 159, 110–118.
- 32 J. S. Stefano, L. O. Orzari, H. A. Silva-Neto, V. N. de Ataíde, L. F. Mendes, W. K. T. Coltro, T. R. Longo Cesar Paixão and B. C. Janegitz, *Curr. Opin. Electrochem.*, 2022, 32, 100893.
- 33 R. C. de Freitas, W. T. Fonseca, D. C. Azzi, P. A. Raymundo-Pereira, O. N. Oliveira and B. C. Janegitz, *Microchem. J.*, 2023, 191, 108823.
- 34 L. R. Sousa, L. C. Duarte and W. K. T. Coltro, *Sens. Actuators, B*, 2020, 312, 128018.
- 35 M. d. L. Reyes-Escogido, E. G. Gonzalez-Mondragon and E. Vazquez-Tzompantzi, *Molecules*, 2011, 16, 1253–1270.
- 36 L. López-Carnllo, M. H. Avila and R. Dubrow, *Am. J. Epidemiol.*, 1994, 139, 263–271.
- 37 S. Bodur, S. E. Bodur, S. Gürsoy, M. F. Ayyıldız, B. Kartoğlu, H. Akbıyık, Ö.T. Günkara and S. Bakırdere, *Microchem. J.*, 2025, 208, 112246.
- 38 L. H. M. AlNahwa, H. M. Ali, T. H. A. Hasanin, K. Shalaby, M. S. Alshammari, A. M. Alsirhani and S. H. Mohamed, *Molecules*, 2024, 29, 2732.
- 39 P. B. Deroco, O. Fatibello-Filho, F. Arduini and D. Moscone, *Electrochim. Acta*, 2020, 354, 136628.
- 40 R. D. Crapnell and C. E. Banks, *Talanta Open*, 2021, 4, 100065.
- 41 I. V. S. Arantes, R. D. Crapnell, E. Bernalte, M. J. Whittingham, T. R. L. C. Paixão and C. E. Banks, *Anal. Chem.*, 2023, 95, 15086–15093.
- 42 R. T. Kachosangi, G. G. Wildgoose and R. G. Compton, *Analyst*, 2008, 133, 888–895.
- 43 W. Lyu, X. Zhang, Z. Zhang, X. Chen, Y. Zhou, H. Chen, H. Wang and M. Ding, *Sens. Actuators, B*, 2019, 288, 65–70.
- 44 I. Jiménez, C. Pérez-Ràfols, N. Serrano, M. del Valle and J. M. Díaz-Cruz, *Microchem. J.*, 2023, 191, 108747.
- 45 Y. Ya, L. Mo, T. Wang, Y. Fan, J. Liao, Z. Chen, K. S. Manoj, F. Fang, C. Li and J. Liang, *Colloids Surf., B*, 2012, 95, 90–95.
- 46 X. Chen, T. Xie, Z. Wang and Q. Gu, *Food Chem.*, 2024, 450, 139257.